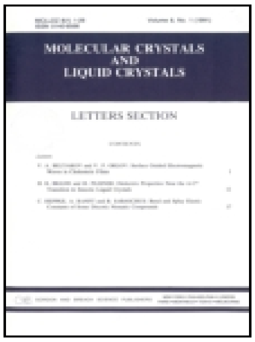

Taylor & Francis
Taylor & Francis Group

Molecular Crystals and Liquid Crystals

ISSN: 1542-1406 (Print) 1563-5287 (Online) Journal homepage: http://www.tandfonline.com/loi/gmcl20

A Simple Synthesis, Characterization, and Properties of Poly(methyl methacrylate) Grafted CdTe Nanocrystals

Xuan Thang Cao, Long Giang Bach, Md. Rafiqul Islam & Kwon Taek Lim

To cite this article: Xuan Thang Cao, Long Giang Bach, Md. Rafiqul Islam & Kwon Taek Lim (2015) A Simple Synthesis, Characterization, and Properties of Poly(methyl methacrylate) Grafted CdTe Nanocrystals, Molecular Crystals and Liquid Crystals, 618:1, 111-119, DOI: 10.1080/15421406.2015.1076305

To link to this article: http://dx.doi.org/10.1080/15421406.2015.1076305

Mol. Cryst. Liq. Cryst., Vol. 618: pp. 111–119, 2015
Copyright © Taylor & Francis Group, LLC
ISSN: 1542-1406 print/1563-5287 online
DOI: 10.1080/15421406.2015.1076305

A Simple Synthesis, Characterization, and Properties of Poly(methyl methacrylate) Grafted CdTe Nanocrystals

XUAN THANG CAO,[1] LONG GIANG BACH,[1,2,*]
MD. RAFIQUL ISLAM,[1] AND KWON TAEK LIM[1,*]

[1]Department of Imaging System Engineering, Pukyong National University,
Busan, Republic of Korea
[2]Center for Advanced Materials Research, Nguyen Tat Thanh University,
Ho Chi Minh City, Vietnam

A facile chemical synthesis of poly(methyl methacrylate) (PMMA) grafted CdTe nanocrystals (CdTe NCs) has been realized. Initially, CdTe NCs were prepared in a controlled manner using 2-mercaptoehanol (ME) as a capping agent. Then, 3-(trimethoxysilyl) propyl methacrylate having C═C double bonds were anchored with ME capped CdTe NCs through condensation reaction. Subsequently, AIBN initiated in situ *free radical polymerization provided PMMA-*g*-CdTe nanohybrids. The FT-IR investigation suggested the formation of robust covalent bonding between CdTe NCs and the organic PMMA segment. XPS analysis also confirmed PMMA-*g*-CdTe nanohybrids. The physical structure and morphology of the as-prepared nanohybrids were studied by XRD and TEM. The thermal stability of the hybrids was enhanced in comparison with pure PMMA as indicated by TGA analysis. The UV-Vis absorption and photoluminescence measurements of the PMMA-*g*-CdTe nanohybrids showed their potential optical properties.*

Keywords CdTe nanocrystals; PMMA-*g*-CdTe nanocomposites; optical properties.

1. Introduction

Semiconductor nanocrystals (NCs), so called quantum dots (QDs), have attracted extensive interest because of their size-dependent optical and electrical properties [1,2]. Over the decades, CdTe NCs have been substantially studied in industrial and biomedical applications, such as light-emitting devices (LEDs), photovoltaic devices, solar cells, biological labels and detection [3–5]. Compared with the organic dyes, CdTe NCs have a wide range of selected wavelengths, continued absorption spectra, great luminescence lifetime, good stability under relatively harsh environments, and small full width at half maximum (FWHM) [6–9]. As a result, a wide variety of synthetic methods for the preparation of CdTe NCs have been developed. Although the water-based syntheses are relatively fast and simple but

---

[*]Address correspondence to Long Giang Bach and Kwon Taek Lim, Department of Imaging System Engineering Pukyong National University, Busan 608-737, Korea (ROK). E-mail: blgiang@ntt.edu.vn; ktlim@pknu.ac.kr

Color versions of one or more of the figures in the article can be found online at www.tandfonline.com/gmcl.

the hot-matrix syntheses in organic solvents produce NCs of higher quality. The desired properties of the hybrids primarily depend on the uniform dispersion of nanoparticles in polymer matrices [10,11]. So far, in order to prepare hybrid materials with novel properties, CdTe NCs have been incorporated in various polymers, glasses and organic semiconductors [12–14]. To use these highly fluorescent NCs in real applications, it is crucial that the inherently instable QDs are stabilized using inert inorganic or organic materials as matrices. Stabilizing these NCs provides effective dispersion in polymer matrices and allows the optical properties of NCs almost unaltered. Covalent immobilization of polymers onto nanomaterials delivered better dispersion with desired properties than physical blending did. Generally, there are two chemical grafting strategies for the covalent fabrication of nanohybrids, one is covalent attachment of end functionalized polymers to a reactive surface ("grafting to"), and the other is *in situ* polymerization with growth of polymer chains from immobilized initiators ("grafting from") [15–18].

On the other hand, poly(methyl methacrylate) (PMMA) is an important thermoplastic material. It is widely used as optical lenses, fluorescent solar collections and sheet glazing materials because of its optical clarity. QDs embedded in PMMA is a fascinating approach for optoelectronic (LEDs, PDs, solar cells) and photonic applications [19,20]. In this work, we present a simple procedure for covalent immobilization of PMMA on CdTe NCs (PMMA-*g*-CdTe) via *in situ* "grafting from" polymerization strategy. Firstly, hydroxyl-coated CdTe NCs were prepared by a wet chemical route. Then, PMMA-*g*-CdTe nanohybrids were obtained by *in situ* free radical polymerization using 3-(trimethoxysilyl)propylmethacrylate (MPS) functionalized CdTe NCs. The synthesized nanohybrids were investigated by respective spectral and microanalyses techniques.

2. Experimental

Materials

Methyl methacrylate (MMA) was purified by passing the liquid through a neutral alumina column to remove the inhibitor prior to use. 2,2′-Azobisisobutyronitrile (AIBN) was purified by recrystallization from methanol. $CdCl_2 \cdot 2.5H_2O$, sodium tellurite (Na_2TeO_3), 2-mercaptoehanol (ME) and 3-(trimethoxysilyl) propyl methacrylate (MPS) were used as received. De-ionized water was used in all experiments, and all of the other chemicals were of analytical grade. All of the above chemicals were purchased from Sigma Aldrich, Yongin, Korea.

Preparation of Hydroxyl-coated CdTe NCs

In the experiment, $CdCl_2 \cdot 2.5H_2O$ (0.69 g) and ME (0.56 g) were dissolved in 50 mL of distilled water, followed by adjusting the pH to 9 with dropwise addition of NaOH (1 M). Na_2TeO_3 (0.33 g) was dissolved in 50 mL of distilled water and mixed with the Cd^{2+} solution under vigorous stirring at 90°C for 5 h, a yellow brown solution of ME capped CdTe NCs was obtained.

Functionalization of CdTe NCs with MPS

The anchoring of MPS on the surface of CdTe NCs is as follows: after dispersing 0.50 g of CdTe-OH NCs in 20 mL of DMF, 0.75 g of MPS was added, and the resulting solution was stirred vigorously under nitrogen at 110°C for 12 h. Toluene was used as the precipitant

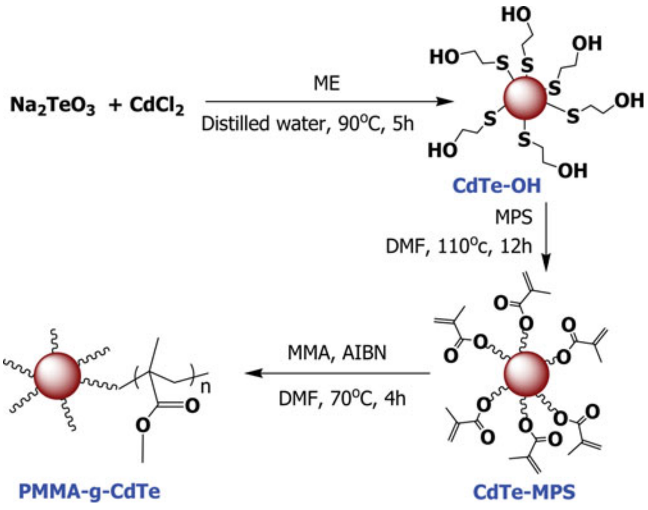

Scheme 1. Synthetic protocol of PMMA-*g*-CdTe nanohybrids.

to obtain MPS tethered CdS NCs, and then the product was washed with fresh DMF for several times. Finally, the product was dried at 30°C for 24 h under vacuum.

*Synthesis of PMMA-*g*-CdTe NCs Nanohybrids*

A typical procedure for the synthesis of PMMA-*g*-CdTe nanohybrids is as follows: 1.0 g of MMA, 0.1 g of CdTe-MPS, 0.01 g of AIBN and 3.0 mL of DMF were placed in a 25 mL round flask equipped with a reflux condenser. The flask was purged with nitrogen, heated to 70°C and kept stirring for 4 h. After the reaction, the flask was cooled to room temperature and the reaction mixture was precipitated in a large excess of hexane. The product was washed with toluene for several times and dried at 30°C for 24 h under vacuum.

Measurements

Fourier-transformed infrared (FT-IR) spectra were recorded to identify the chemical bonds in the surface of nanohybrids using a BOMEM Hartman & Braun FT-IR spectrometer. Surface composition was investigated by X-ray Photoelectron Spectroscopy (XPS, Thermo VG Multilab 2000). Transmission Electron Microscopy (TEM) images were captured using a Joel JEM 2010 instrument. The crystallographic state of the samples was determined by a Philips X'pert-MPD. Thermogravimetric analysis (TGA) was conducted with a Perkin-Elmer Pyris 1 analyzer (USA). Photoluminescence (PL) spectra were recorded by an F-4500 spectrofluorometer (Hitachi, Japan) at 360 nm. Ultraviolet–visible (UV–Vis) absorption spectra were recorded on a himadzu UV-1800 UV-Vis Spectrophotometer in the range of 400–750 nm.

3. Results and Discussion

The synthetic route for the preparation of hydroxyl group coated CdTe NCs and PMMA-*g*-CdTe nanohybrids is outlined in Scheme 1. The effective grafting of MPS on CdTe NCs and the synthesis of PMMA-*g*-CdTe nanohybrids are evident from the FT-IR data

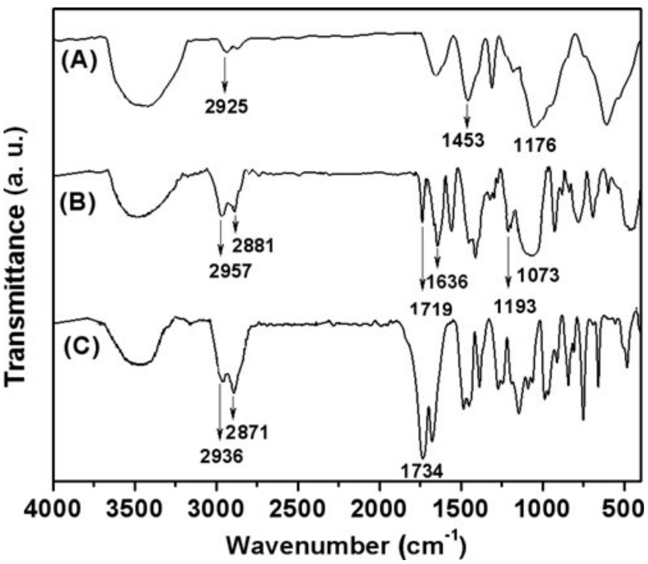

Figure 1. FT-IR spectra of (A) CdTe-OH NCs, (B) MPS functionalized CdTe NCs and (C) PMMA-*g*-CdTe nanohybrids.

of functionalized NCs powder. Fig. 1 depicts the FT-IR spectra of hydroxyl coated CdTe NCs, MPS-functionalized CdTe NCs and PMMA-*g*-CdTe nanohybrids. In the spectrum of MPS functionalized CdTe NCs (Fig. 1B), the absorptions at 2957, 2881, 1719, 1193 and 1073 cm^{-1} correspond to the stretching vibration of CH_3, CH_2, C=O, C−O−C and Si−O−C groups of MPS, respectively. [17] In addition, the absorption at 1636 cm^{-1} is the characteristic absorption of the C=C double-bond in the functionalized CdTe NCs after the condensation reaction. It is speculated that the MPS tethered CdTe NCs are highly compatible in PMMA matrices. In Fig. 1C, a new absorption band at 1734 cm^{-1} is assigned to the C=O stretching vibration of PMMA. The bands in the range of 3000–2850 cm^{-1} are assigned to the C−H stretching vibrations of the CH_3 and CH_2 groups of grafted PMMA. [19] The above data suggest that PMMA is covalently grafted on the surface of CdTe NCs.

XPS was employed to investigate the surface chemical composition of CdTe-OH, MPS functionalized CdTe NCs and PMMA-*g*-CdTe nanohybrids. Fig. 2A shows the XPS spectrum of CdTe-OH which is dominated by signals attributable to Cd, Te, C, O and S. The immobilization of the MPS moiety on the surface of CdTe NCs is suggested by the characteristic signals of Cd_{3s} (772.9 eV), Cd_{3p1} (658.6 eV), Cd_{3p3} (624.5 eV), Te_{3d3} (593.7 eV), Te_{3d5} (583.1 eV), O_{1s} (538.6 eV), Cd_{3d} (412.21 eV), C_{1s} (292.2 eV), S_{2s} (232.5), S_{2p} (168.6 eV), Te_{4p} (116.1 eV) and Si_{2p} (102.4 eV) (Fig. 2B). The silane coupling agent, MPS immobilized on CdTe NCs can initiate a condensation reaction to afford a stable initiator monolayer, which is consistent with the appearance of the Si signals in the wide-scan spectrum of MPS functionalized CdTe. The XPS scan of PMMA-*g*-CdTe nanohybrids shows that the C_{1s} peak with high intensity slightly shifted to the higher binding energy (BE) indicating that the polymer chains are anchored to the surface of CdTe-OH. The C_{1s} core-level spectra of PMMA-*g*-CdTe nanohybrids are curve-fitted with three peak components having BEs at about 284.6, 286.1 and 288.5 eV attributable to the CH_2/CH_3, C-O and O = C−O species of PMMA, respectively (Fig. 2D).

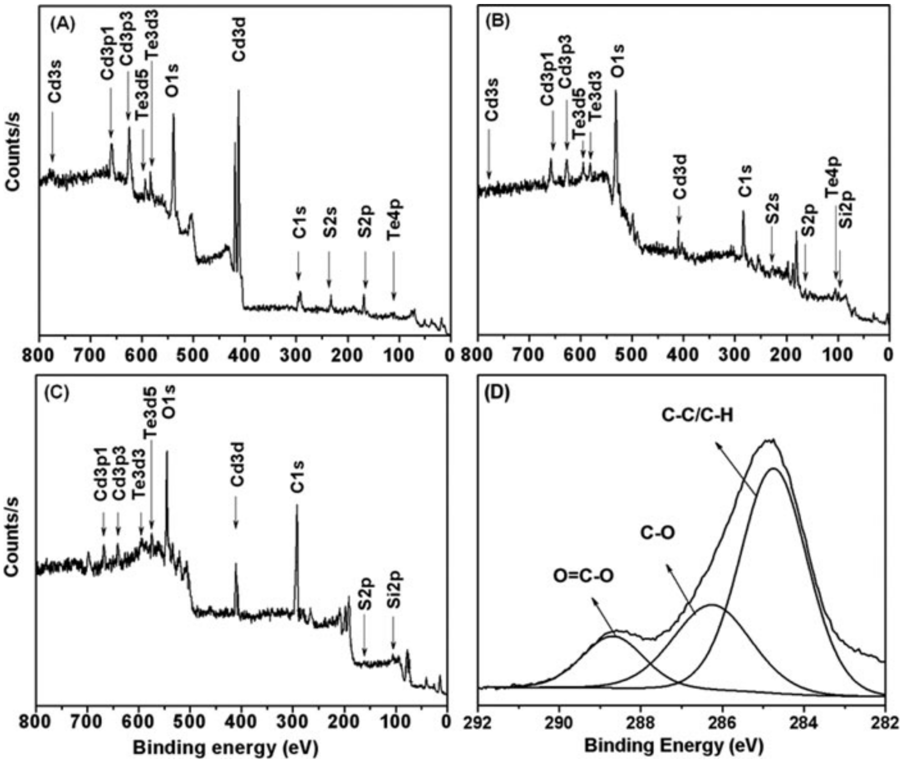

Figure 2. Wide-scan spectra of (A) CdTe-OH, (B) MPS functionalized CdTe NCs, (C) PMMA-*g*-CdTe and (D) C1s core-level spectra of PMMA-*g*-CdTe nanohybrids surface.

The X-ray diffraction pattern of the hydroxyl capped CdTe NCs (Fig. 3A) exhibits main peaks at 2θ values of 25.2°, 38.6°, 46.5 and 56.6° corresponding to the crystal planes (111), (220), (311) and (400) suggesting the zincblende structure of CdTe NCs. [21] The data are in good agreement with the reported CdTe NCs peaks (JCPDS card no. 15-0770). [22] The pattern for the PMMA-*g*-CdTe nanohybrids (Fig. 3C) shows the peaks at almost similar position to those observed in CdTe NCs but its intensity decreases. However, the (400) peak almost disappears. All these results suggest that PMMA is introduced to the crystalline structure of CdTe QDs.

TEM was used to observe the morphology of PMMA-*g*-CdTe nanohybrids. Fig. 4A-B demonstrates the typical TEM images of the synthesized PMMA-*g*-CdTe nanohybrids. It is observed that CdTe NCs are almost well distributed within the PMMA polymer matrices. It suggests that due to the evaporation of solvent a little agglomeration of NCs happens. The average size of the CdTe-OH NCs is estimated to be *ca.* 5 nm. The well-resolved lattice fringes of the CdTe NCs as captured by selected area electron diffraction indicate good crystallinity of the PMMA-*g*-CdTe nanohybrids (Fig. 4C).

The thermal stability of PMMA embedded CdTe NCs was investigated by TGA analysis. Fig. 5 shows the TGA micrographs of the PMMA-*g*-CdTe nanohybrids and pure PMMA. The TGA curve of PMMA-*g*-CdTe nanohybrids reveals a major weight loss in the temperature range from 285 to 430°C, which is possibly due to the presence of significant amount of combustible polymers (Fig. 5B). It is observed that the PMMA loses

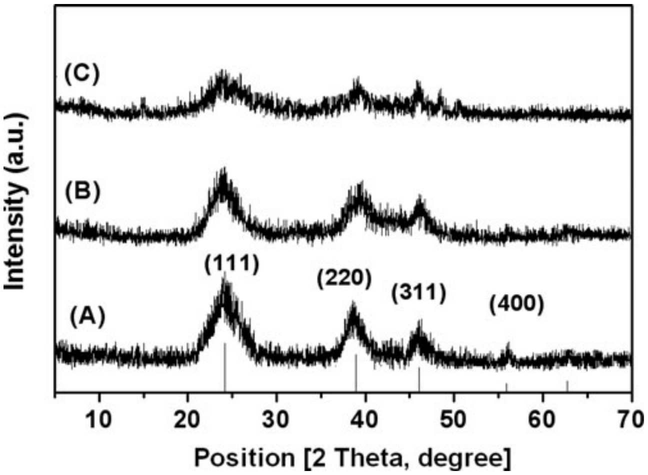

Figure 3. The XRD patterns of (A) CdTe-OH, (B) MPS functionalized CdTe NCs, (C) PMMA-*g*-CdTe nanohybrids.

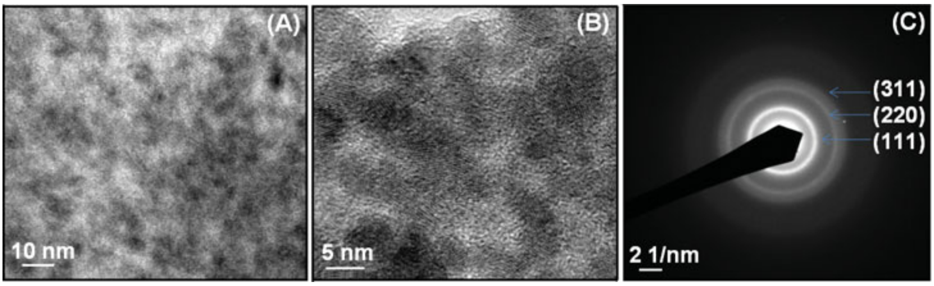

Figure 4. (A, B) TEM images at different magnifications, and (C) the SAED pattern of PMMA-*g*-CdTe nanohybrids.

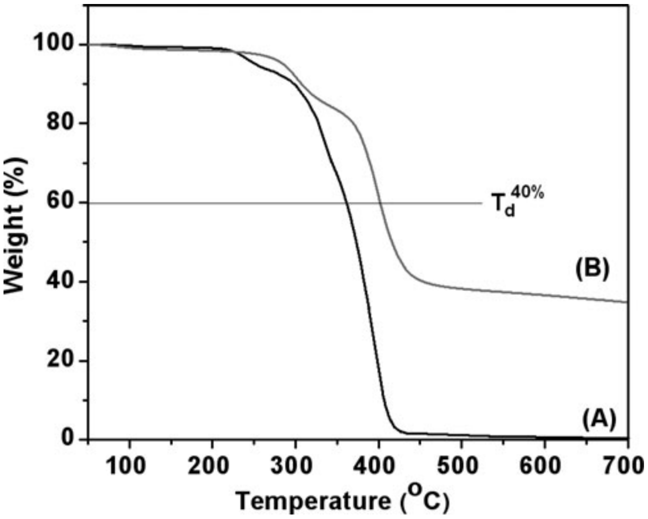

Figure 5. TGA scans of (A) pure PMMA polymer, and (B) PMMA-*g*-CdTe nanohybrids.

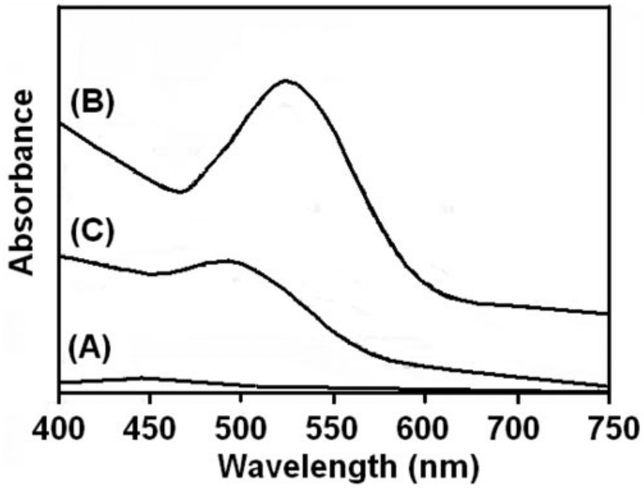

Figure 6. UV–Vis spectra of (A) pure PMMA, (B) hydroxyl-coated CdTe NCs, and (C) PMMA-*g*-CdTe nanohybrids.

40% of weight at the decomposition temperature (T_d) of 368°C, on the contrary PMMA-*g*-CdTe nanohybrids lose the same weight at T_d of 412°C. The char yields of the MMA and PMMA-*g*-CdTe nanohybrids at 700°C are 0.7% and 34.1%, respectively. The TGA curve of the nanohybrid shows the presence of residual amount of inorganic CdTe NCs. It can be explained such a way that the interaction between CdTe NCs and the PMMA matrix are so strong that the thermal degradation of PMMA is much difficult. This result suggests that PMMA-*g*-CdTe nanohybrids are thermally more stable, and nanohybrids can be stored for a long time without deterioration under ambient condition.

To investigate the optical properties of PMMA-*g*-CdTe nanohybrids, UV-Vis absorption and PL spectroscopy were employed. The absorption maximum of CdTe NCs was found to be 523 nm. On the other hand, the as-prepared nanohybrids displayed the absorption maximum at 498 nm which was observed to be blue shifted comparing with the CdTe NCs. Moreover, PMMA was less sensitive towards the UV-Vis excitation (Fig. 6A). The results indicate that the CdTe NCs retain its optical property upon being hybridized. Fig. 7 shows the PL emission spectra of pure PMMA, hydroxyl-coated CdTe NCs and PMMA-*g*-CdTe nanohybrids with excitation at 360 nm. As seen in Fig. 7A, there is no obvious PL sensitivity in pure PMMA, whereas a strong emission peak at 572 nm can be observed in CdTe NCs (Fig. 7B), exhibiting a well-defined excitonic emission feature. Fig. 7C shows that the PL intensity of PMMA-*g*-CdTe nanohybrids was enhanced by a little red shift (581 nm). This phenomenon happened due to the decrease of surface defects upon PMMA grafting on CdTe NCs. As it is widely believed that broad peak in the visible region is associated with the structural defects like interstitials, tellurium vacancies and surface traps on the QDs. In the case of CdSe QDs, surface states such as dangling bonds are usually involved in non-radiative processes, while Te^{2-} ions provide a critical pathway for the visible emission band. The PMMA immobilization reduces the density of surface dangling bonds and Te^{2-} ions, so that the probability of non-radiative transitions is further reduced thereby increasing the probability of visible emission. It is known that the reduction of surface defects prevents non-radiative recombination of electrons and holes resulting in the increase of fluorescence efficiency. This approach of devising chemically

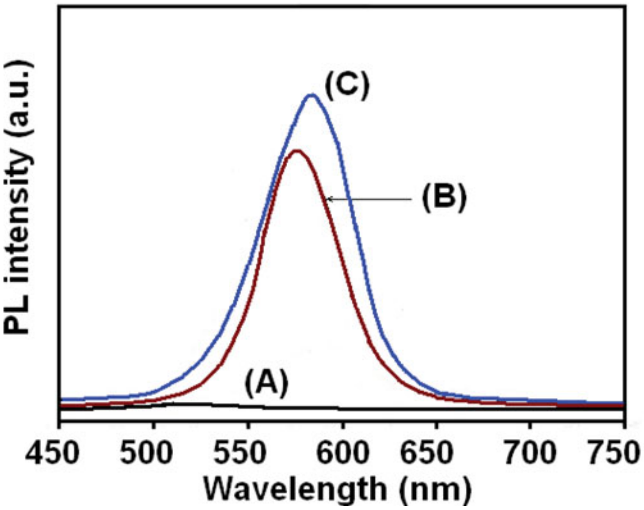

Figure 7. PL spectra of (A) pure PMMA, (B) hydroxyl-coated CdTe NCs, and (C) PMMA-*g*-CdTe nanohybrids.

grafted NCs for fabricating smart optical devices will find wide applications in optical plastic, optoelectronics, or biological labeling.

Conclusions

PMMA anchored CdTe NCs (PMMA-*g*-CdTe) were synthesized by *in situ* free radical polymerization of MMA from the MPS immobilized CdTe NCs. The strong chemical bond between PMMA and MPS capped CdTe NCs was suggested by FT-IR analysis. The XPS mapping analysis also demonstrated the successful preparation of PMMA-*g*-CdTe nanohybrids. The XRD analysis of the PMMA ligated CdTe NCs suggested a zincblende cubic phase structure. The CdTe NCs were found to be well dispersed in polymer matrices as observed from TEM images. The size of CdTe NCs was observed to be *ca.* 5 nm from TEM. At 40% weight loss, the decomposition temperature of PMMA was found at 368°C while PMMA-*g*-CdTe demonstrated decomposition at 412°C as calculated from TGA scan. The PL intensity of PMMA-*g*-CdTe nanohybrids was higher than CdTe NCs, which might be due to the reducing of surface defects of NCs by PMMA.

Acknowledgment

This work was supported by the BK21 Plus program.

References

[1] Cao, X. D., Li, C. M., & Bao, H. F. (2007). *Chem. Mater.*, *9*, 3773.
[2] Adamczaka, M., Hoel, H. J., Gaudernack, G., Barbasz, J., Szczepanowicza, K., & Warszynski, P. (2012). *Colloids Surf., B*, *90*, 211.
[3] Meier, R., Word, R. C., Nadarajah, A., & Könenkamp, R. (2008). *Phys. Rev. B.*, *77*, 195314.
[4] Lan, G. Y., Yang, Z., Lin, Y. W., Lin, Z. H., Liao, H. Y., & Chang, H. T. (2009). *J. Mater. Chem.*, *19*, 2349.

[5] Liu, X., Jiang, H., Lei, J., & Ju, H. (2007). *Anal. Chem.*, *79*, 8055.

[6] Datta, J., Jana, A., & Bhattacharya, C. (2009). *Electr. Acta.*, *54*, 5470.

[7] Zhong, H. Z., Zhou, Y., & Yang, Y. (2007). *J. Phys. Chem. C.*, *111*, 6538.

[8] Shen, J. M., Tang, W. J., Zhang, X. L., Chen, T., & Zhang, H. X. (2012). *Carbohydrate Polym.*, *88*, 239.

[9] Tomasulo, M., Yildiz, I., & Kaanumalle, S. L. (2006). *Langmuir*, *22*, 10284.

[10] Kim M. J., Chae H. S. & Choi H.J. (2015). *J. Ind. Eng. Chem.*, *21*, 145.

[11] Bach, L. G., Islam, M. R., Kim, J. T., Seo, S. Y., & Lim, K. T. (2012). *Appl. Surf. Sci.*, *258*, 2959.

[12] Tamborra, M., Striccoli, M., Comparelli, R., Curri, M. L., Petrella, A., & Agostiano, A. (2004). *Nanotechnology*, *15*, S240.

[13] Skirtach, A. G., Dejugnat, C., Braun, D., Susha, A. S., Rogach, A.L., & Sukhorukov, G. B. (2007). *J. Phys. Chem. C*, *111*, 555.

[14] Mokari, T., Sertchook, H., Aharoni, A., Ebenstein, Y., Avnir, D., & Banin, U. (2005). *Chem. Mater.*, *17*, 258.

[15] Kim, J. Y., Ihn, K. J., & Na, J. S. (2011). *J. Ind. Eng. Chem.*, *17*, 248.

[16] Ye, S., Shen, C., Pang, H., Wang, J., & Lu, Y. (2011). *Polymer*, *52*, 2542.

[17] Guo, L., Chen, S., & Chen, L. (2007). *Colloid. Polym. Sci.*, *285*, 1593.

[18] Mittal G., Dhand V., Rhee K. Y., Park S. J. & Lee W. R. (2015). *J. Ind. Eng. Chem.*, *21*, 11.

[19] Song, H., & Lee, S. (2007). *Nanotechnology 18*, 055402.

[20] Chung, W., Park, K., Yu, H. J., Kim, J., Chun, B. H., & Kim, S. H. (2010). *Opti. Mater.*, *32*, 515.

[21] Hwang, C. H., Park, J., Song, M., Lee, J. H., & Shim, I. W. (2011). *Bull. Korean Chem. Soc.*, *32*, 2207.

[22] Liu, J. G., Liang, J. G., Han, H. Y., & Sheng, Z. H. (2009). *Mater. Lett.*, *63*, 2224.